Available online at www.sciencedirect.com
SCIENCE DIRECT
Journal of Power Sources 158 (2006) 747–753
JOURNAL OF POWER SOURCES
www.elsevier.com/locate/jpowsour

Evaluation of different approaches for improving the cycle life of MgNi-based electrodes for Ni-MH batteries

C. Rongeat, M.-H. Grosjean, S. Ruggeri, M. Dehmas, S. Bourlot, S. Marcotte, L. Roué *

INRS-Énergie, Matériaux et Télécommunications, 1650 Blvd. Lionel-Boulet, Varennes, Que., Canada J3X 1S2

Received 4 August 2005; received in revised form 2 September 2005; accepted 6 September 2005
Available online 18 October 2005

Abstract

Several methods have been investigated to enhance the cycle life of amorphous MgNi used as the negative electrode for Ni-MH batteries. The first approach involves modifying its surface composition in different ways, including the electroless deposition of a chromate conversion coating, the addition of chromate salt or NaF into the electrolyte and the mechanical coating of the particles with various compounds (e.g. TiO_2). Another approach consists of developing ($MgNi + AB_5$) composite materials. However, the cycle life of these modified MgNi electrodes remains unsatisfactory. On the other hand, the modification of the bulk composition of the MgNi alloy with elements such as Ti and Al appears to be more effective. For instance, a $Mg_{0.9}Ti_{0.1}NiAl_{0.05}$ electrode retains 67% of its initial discharge capacity (404 mAh g^{-1}) after 15 cycles compared to 29% for MgNi. The charging conditions also have a great influence on the electrode cycle life as demonstrated by the existence of a charge input threshold below which minor capacity decay occurs. In addition, the particle size has a major influence on the electrode performance. We have developed an optimized electrode constituted of $Mg_{0.9}Ti_{0.1}NiAl_{0.05}$ particles with the appropriate size (>150 μm) showing a capacity decay rate as low as ∼0.2% per cycle when charged at 300 mAh g^{-1}.

Keywords: Nickel-metal hydride battery; Hydrogen storage alloys; Magnesium-based compounds; Mechanical alloying; Cycle life

1. Introduction

Magnesium-based alloys exhibit promising properties as negative electrode materials for nickel-metal hydride (Ni-MH) batteries. For instance, amorphous MgNi obtained by mechanical alloying has an initial discharge capacity close to 500 mAh g^{-1} [1] compared to ∼300 mAh g^{-1} for $LaNi_5$-type alloys used in commercial Ni-MH batteries. Nevertheless, MgNi alloy is not satisfactory for practical use since a capacity decay of 70% is observed after only 20 charge/discharge cycles. This rapid deterioration upon cycling is related to the alloy oxidation/pulverization process. Indeed, by reacting with the KOH electrolyte, magnesium is easily oxidized to $Mg(OH)_2$, which limits the hydrogen absorption/desorption reaction in addition to consuming active material [2–5]. This oxidation is strongly accelerated by the pulverization of the MgNi particles [6] which is related to their volume expansion upon hydrogen charging, generating new surfaces to be oxidized by the electrolyte.

In the last few years, numerous studies have been conducted in order to improve the cycle life of MgNi-based materials. Up to now, the most promising results have been obtained by the partial substitution of magnesium by corrosion resistant elements such as Ti. For example, amorphous $Mg_{0.7}Ti_{0.3}Ni$ alloy retains 92% of its initial discharge capacity of 325 mAh g^{-1} after 20 cycles [7]. However, the global performance of the Mg-based electrodes is still far from that required for commercial application.

In the present study, several ways for improving the cycle life of the MgNi electrode have been evaluated, as summarized in Fig. 1. These include coating the alloy surface, modifying the electrolyte composition, the elaboration of composite materials, the modification of the bulk composition of the alloy, powder sieving, and control of the charge input. By combining some of

* Corresponding author. Tel.: +1 450 929 8185; fax: +1 450 929 8102.
E-mail address: roue@emt.inrs.ca (L. Roué).

0378-7753/$ – see front matter © 2005 Elsevier B.V. All rights reserved.
doi:10.1016/j.jpowsour.2005.09.006

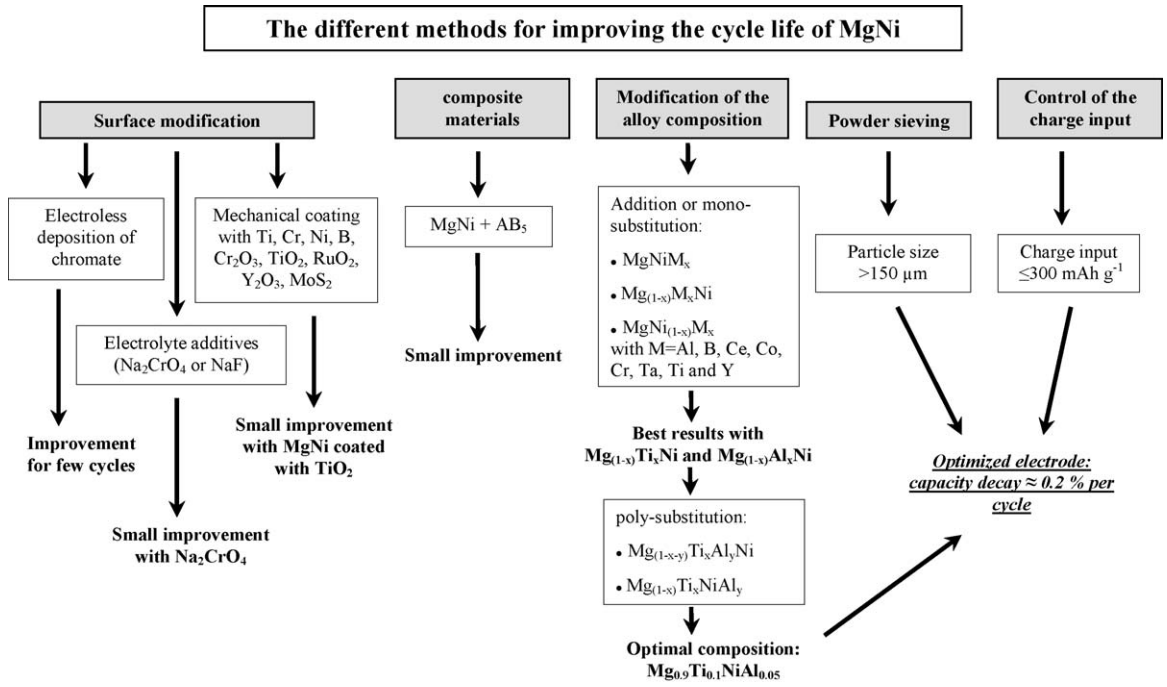

Fig. 1. The different approaches evaluated in the present study for improving the cycle life of the amorphous MgNi electrode.

these modifications, an optimized MgNi-based material with a long cycle life has been obtained.

2. Experimental

Amorphous MgNi alloy and its derivatives were prepared by mechanical alloying. Pure elements were introduced into a steel vial under Ar atmosphere. Three steel balls (two with 11 mm diameter and one with 14 mm diameter) were added with a ball-to-powder mass ratio of 10:1. Ball milling was performed using a Spex 8000 vibratory mill for 10 h. The amorphous structure of the end-products was confirmed by X-ray diffraction analyses (not shown). X-ray photoelectron spectroscopy (XPS) analyses were performed using a VG Escalab 220I-XL with a monochromatic Al Kα source. The C 1s peak at 284.6 eV was used as an internal reference to calibrate the peak positions.

Electrochemical charge/discharge cycling tests were performed on an Arbin BT2000 battery tester at room temperature in a 6 M KOH electrolyte using a three-electrode cell. The working electrode was composed of 100 mg active material with 800 mg of graphite and 20 mg of carbon black. The counter electrode was a nickel wire and the reference electrode was a Hg/HgO electrode. The working electrode was charged at 200 mA g^{-1} for 3 h and discharged at 20 mA g^{-1} with a cut-off potential fixed at −0.6 V. The influence of the charge input was studied by varying the charge duration from 60 to 90 min, corresponding to a charge input varying from 200 to 300 mAh g^{-1}.

3. Results and discussion

3.1. Electroless deposition

The corrosion behavior of magnesium and its alloys has been largely investigated in various environments and is still an active field of research in corrosion science [8]. Significant improvements in the corrosion resistance of Mg have been achieved by reducing the metal impurity content (i.e. prevention of internal galvanic attacks) or by alloying with elements such as aluminum or rare earth elements. Another effective and simple way to prevent Mg corrosion is to coat it with a protective layer. Such a coating can protect the substrate by acting as a barrier between the metal and its environment and/or by containing corrosion inhibiting compounds. Electrochemical plating, conversion coating, anodizing, hydride coatings, organic coatings and vapor-phase processes can be used for coating Mg and its alloys [9]. Each of these methodologies has their own advantages and disadvantages. For the present purpose, the protective layer must be effective in KOH without inhibiting the hydrogen diffusion and electron transfer reactions. Chromate conversion coating appears as a good candidate since such a protective layer is generally thin and stable in alkaline media. Chromate conversion coatings on magnesium consist of a dense layer of Mg(II) and Cr(III) hydroxides covering the Mg surface with a porous overlayer of $Cr(OH)_3$ [10]. Several dip and anodizing processes exist to form chromate conversion coatings on Mg-based materials [11].

In the present case, chromate coating was performed by electroless deposition: 200 mg of MgNi powder were immersed in 20 mL of a solution composed of $Na_2Cr_2O_7{\cdot}2H_2O$ (90 g L^{-1}) and HNO_3 (96 g L^{-1}). This mixture was then stirred for 4 min at room temperature. Finally, the powder was rinsed with pure water and dried at 60 °C in air. After treatment, XRD and XPS analyses were performed. From the XRD analysis (not shown), no new XRD peaks corresponding to Cr-based compounds are observed, suggesting that the deposited layer is thin. On the other hand, the formation of a chromate conversion coating on the MgNi particles is revealed by XPS analysis with Cr $2p_{3/2}$

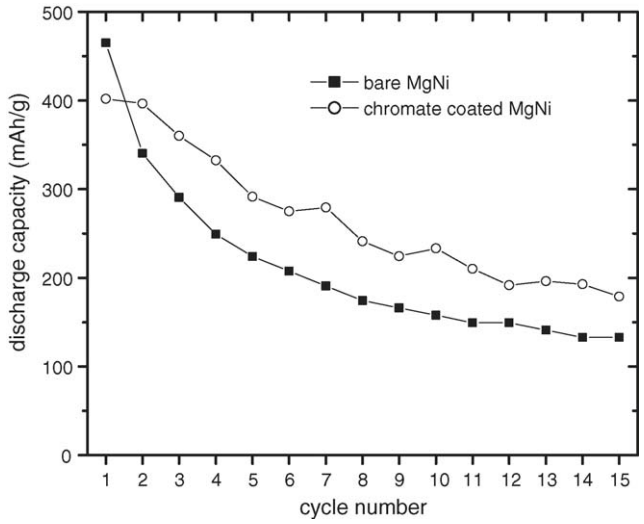

Fig. 2. Cycling discharge capacities of bare MgNi and chromate-coated MgNi electrodes.

and Cr $2p_{1/2}$ peaks observed at 577.1 and 587.0 eV, respectively. They are assigned to a combination of Cr(III) and Cr(VI) [12] in a proportion of about 75/25. On the basis of the Mg 1s, Ni 2p and Cr 2p peaks, the surface concentrations of Mg, Cr and Ni are estimated to be 52, 42 and 6%, respectively (oxygen was not considered in the calculation).

The cycling dischargeability of bare MgNi and chromate-coated MgNi electrodes is shown in Fig. 2. The surface-modified MgNi electrode displays a lower initial capacity (402 mAh g^{-1}) compared to the untreated electrode (465 mAh g^{-1}). This may be related to some Mg oxidation during the deposition process and because the chromate conversion coating may limit the surface hydriding/dehydriding process. It may also reflect the absence of additional discharge capacity related to the anodic formation of $Mg(OH)_2$ upon discharge [6] due to the presence of the protective chromate conversion layer. This protective action of the chromate coating against Mg oxidation is effective during the two first charge/discharge cycles. Unfortunately, the capacity decay thereafter is almost the same for untreated and coated MgNi electrodes. This can be explained by the rupture of the chromate conversion layer due to the pulverization of the particles upon cycling, creating new and unprotected surfaces which are promptly oxidized by the electrolyte. Thus, the approach which consists of protecting the powder with a dense surface layer is not appropriate for metal hydride materials having an extended volume expansion upon hydrogen absorption, since this induces an enormous mechanical stress in the coating. This agrees with several studies showing the unsatisfactory improvement of the cycle life of Mg-based alloys coated by electroless plating of Cu [13], Ni [14] and Ni-alloys [15]. In contrast, the electroless coating of Cu [16], Co [17,18] and Ni [19] on $LaNi_5$-based alloys appears more effective for improving the electrode cycle life, maybe because of the lower stress-cracking of these optimized metal hydrides. Thus, a decrease of the pulverization of the Mg-based alloys is required before considering its surface modification by a protective film.

Table 1
The 1st and 10th cycle discharge capacities of MgNi with respect to the chromate concentration in the electrolyte

Chromate content (g L^{-1})	0	1	10	20	50
C_1 (mAh g^{-1})	465	407	371	258	179
C_{10} (mAh g^{-1})	158	164	176	146	108
C_{10}/C_1 (%)	34	40	47	57	60

3.2. Electrolyte additive

As shown previously, coated Mg-based alloys suffer from the rupture of the protective surface layer due to the expansion/contraction of the particles upon cycling. In order to reduce this problem, in situ modification of the surface of the MH particles upon cycling has been tested. For that purpose, the electrolyte was modified by adding chromate salt $Na_2Cr_2O_7{\cdot}2H_2O$ to the 6 M KOH solution. It is expected that the deposition of a protective chromate layer may occur continuously on the freshly fractured MgNi particles. As shown in Table 1, the presence of chromate ions in the electrolyte has a positive effect on the electrode cycle life since the capacity retention measured after 10 cycles (C_{10}/C_1) increases with the chromate concentration. However, at the same time, the initial discharge capacity decreases substantially, probably due to an increase of the electrode polarization resistance as the chromate layer becomes thick and dense. Thus, this approach does not appear appropriate for improving MgNi electrode performance. In comparison, in situ Pd electrodeposition on a Mg_2Ni electrode by adding $PdCl_2$ to the electrolyte significantly enhances the cyclic stability and rate capability of the MH electrode without affecting its maximum discharge capacity [20]. However, the Pd-coated Mg_2Ni electrode still lost 40% of its initial capacity (460 mAh g^{-1}) within the first 20 cycles. Besides, Kim et al. [21] have shown that in KOH + KF electrolyte, a continuous and stable fluorinated layer is formed on the Mg_2Ni particles, which leads to an increase of the cycling durability and high-rate dischargeability of the electrode. However, the stabilized capacity of the F-treated Mg_2Ni electrode appears very low (~100 mAh g^{-1}). Note that our experiments performed with amorphous MgNi in 6 M KOH + NaF (0.5–50 g L^{-1}) electrolyte did not show any improvement of the electrode performance.

3.3. Mechanical coating

The surface modification of MgNi-based alloys by milling the parent alloy with an additional element such as Ni [3], Ti [22] or C [23] for a short period (typically, few tens of minutes) effectively reduces the rate of degradation of the electrode upon cycling. This can be explained by the fact that such a surface modification by milling consists of the dispersal of an element on the MH particle surface, thus improving the corrosion resistance of the alloy rather than the formation of a complete and dense coating and hence, it must be less sensitive to the powder expansion upon cycling.

In the present work, amorphous MgNi has been mechanically coated with various pure metals (Cr, Ti, Ni), metalloid (B), metal

oxides (Cr_2O_3, TiO_2, RuO_2, Y_2O_3) and metal disulfide (MoS_2). The study of the optimization of the milling parameters for the preparation of these materials has shown that it is necessary to adjust the quantity of the added element, the milling time, the ball-to-powder mass ratio, the number and size of the balls and the type of miller to reach a good dispersal (checked by EDX mapping) of the additive on the surface of the MgNi powder without modifying its structure (confirmed by XRD analysis). The protocol which appears to be the most adequate consists of milling for 30 min using a Spex vibratory miller, with a moderate quantity (10 wt.%) of added element and a ball-to-powder mass ratio of 20:1 using 10 balls of 8 mm diameter. However, despite a homogeneous distribution of the additives onto the MgNi particles, no major improvement in terms of cycle durability has been obtained. Among the different additives evaluated, the best result was observed on MgNi + 10 wt.% TiO_2, which displays a capacity decay of 50% after 10 cycles compared to 66% for the unmodified MgNi. However, the presence of TiO_2 on the surface of the MgNi alloy has a negative effect on its high-rate dischargeability. In addition, it was observed that the milling of MgNi with a pure metal such as Ti for a period longer than 1 h, leading to the modification of the bulk composition of the parent alloy, is more prone to improve the performance of the electrode. This suggests that the modification of the composition of MgNi by partial substitution/addition is a better way than the surface modification for improving the cycle life of MgNi-based materials, as confirmed below (see Section 3.5).

3.4. Composite materials

Several studies have reported an improvement of the electrochemical hydriding/dehydriding properties of various composite MH materials related to a cooperative phenomena between the different metal hydride phases constituting the electrode [24–30]. For instance, the composite electrode made from a ZrCrNi compound ball milled for 20 min with 5 wt.% amorphous $Mg_{40}Ni_{60}$ alloy displays a considerable increase of its discharge capacity, rate capability and cycle life with respect to that of ZrCrNi alone [24]. Besides, Han et al. [28] have shown an important cycle life improvement for a Mg_2Ni plus TiNi composite material synthesized from elemental Mg, Ni and Ti powders, with a charge retention of 55% after 150 cycles but with a very low maximal capacity ($\sim$130 mAh g^{-1}).

In the present work, composite materials with amorphous MgNi as major phase were produced by milling MgNi with 2–50 wt.% AB_5-type alloy for a milling duration varying from 15 min to 5 h. Our results indicate that a large amount of AB_5-type alloy (50 wt.%) and a short mixing time (30 min) are required to observe an appreciable increase of the cycle life of the composite MH electrode. However, the capacity decay of the composite electrode is still too high (35% after 10 cycles) compared to that measured for a $LaNi_5$-based electrode (2% after 10 cycles). Moreover, the initial discharge capacity of the (50 wt.% MgNi + 50 wt.% AB_5) composite electrode is rather low (325 mAh g^{-1}).

3.5. Modification of the bulk composition

A possible way to increase the cycle life of MgNi is by adjusting its composition by partial substitution of Mg and/or Ni in order to improve its corrosion resistance in the KOH electrolyte and/or to diminish its pulverization upon cycling. The partial substitution of Mg and/or Ni may also have an effect on the charge/discharge capacity and kinetics of the electrode by modifying the metal–hydrogen interaction (electronic effect), by modifying the hydrogen site size (geometric effect) and/or by the formation of additional phases (synergetic effect). Such a partial substitution approach has been successfully applied in the case of AB_5- and AB_2-type alloys.

In the last few years, several research groups have conducted studies on the effect of partial substitution on the electrode performance of MgNi-based hydrogen storage alloys. The choice of the substituting elements (nature and number), the substitution ratio as well as the substituted element (Mg and/or Ni) leads to an infinite number of possible combinations. On the basis of the literature data and in spite of a few contradictory studies, a few elements of substitution can be identified as promising:

(i) *Aluminum*. Kohno and Kanda [31] have demonstrated that it is possible to improve the cycle life of the electrode by using $Mg_{1.9}Al_{0.1}Ni$ rather than Mg_2Ni. This is supported by the work of Jianshe et al. [32] indicating the formation of Al_2O_3 on the surface of an Al-substituted Mg_2Ni electrode that inhibits further corrosion of the alloy.

(ii) *Vanadium*. The improvement of the MgNi cycle life has been observed by the partial substitution of Mg by V. This is explained by the formation of a vanadium oxide layer, which reduces the rate of formation of $Mg(OH)_2$ on the alloy surface during the charge–discharge cycling [33,34].

(iii) *Yttrium*. The partial substitution of Mg with Y enhances the resistance of the alloy against corrosion in alkaline media and increases its cycle life [35].

(iv) *Titanium*. Several works have shown that Ti as partial substitute for Mg in MgNi and Mg_2Ni alloys is effective in improving the electrode cycle life [5,7,36–40]. This is associated with the formation of titanium oxides on the alloy surface that limit further oxidation of Mg and induce a Ni enriched layer on the alloy surface [7]. Moreover, some investigations on polysubstituted MgNi-based materials have demonstrated a synergetic effect between Ti and various elements such as V [33,41], Zr [41–43], Cr [44] and Al [42,45,46]. This is assumed to be associated with the formation of a more compact and more protective composite oxide layer on the electrode surface than with Ti alone.

The present work provides more extensive data about the influence of the partial substitution of Mg and Ni in MgNi on its electrode performance. For that purpose, $MgNiM_x$, $Mg_{1-x}M_xNi$ and $MgNi_{1-x}M_x$ (x varying from 0.05 to 0.5) compounds with M = Al, B, Ce, Co, Cr, Ta, Ti and Y have been evaluated. All these materials were produced from elemental powders milled for 10 h.

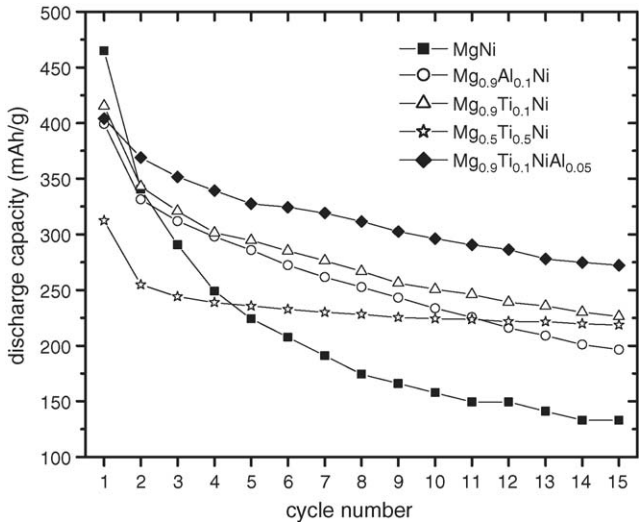

Fig. 3. Cycling discharge capacities of MgNi, $Mg_{0.9}Al_{0.1}Ni$, $Mg_{0.9}Ti_{0.1}Ni$, $Mg_{0.5}Ti_{0.5}Ni$ and $Mg_{0.9}Ti_{0.1}NiAl_{0.05}$ electrodes.

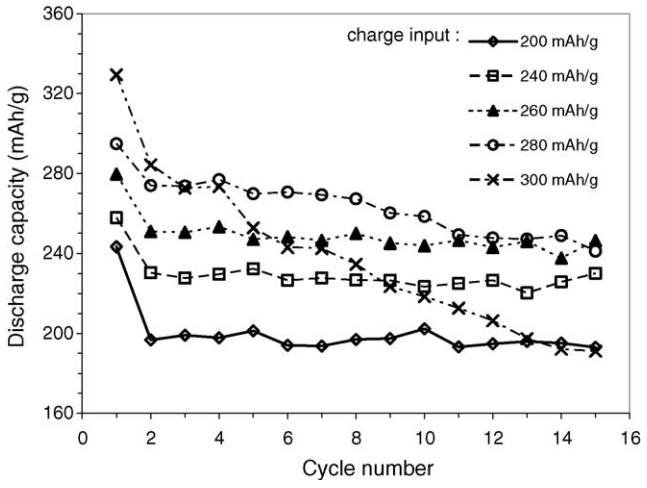

Fig. 4. Cycling discharge capacities of $Mg_{0.9}NiTi_{0.1}Al_{0.05}$ as a function of the charge input.

Our results show that the partial substitution ($x = 0.05$) of Ni by Co, Al and Ti leads to an increase of the initial discharge capacity of about 50 mAh g^{-1} in comparison with unsubstituted MgNi. This might be related to the destabilization of the metal hydride through the partial substitution of Ni, favoring the H desorption process. On the other hand, it appears clear that the partial substitution of Mg is more effective than Ni substitution or element addition for improving the cycle life of the MgNi-based electrodes. This is not surprising since Mg is the corrosion sensitive element in MgNi. Among the different substitutes for Mg, the most efficient elements for improving the electrode cycle life are Ti and Al as illustrated in Fig. 3, where the amorphous compounds $Mg_{0.9}Al_{0.1}Ni$ and $Mg_{0.9}Ti_{0.1}Ni$ display a charge retention of 49 and 54%, respectively, after 15 cycles compared to 29% for MgNi. A substantial enhancement of the capacity retention can be obtained by increasing the amount of the Mg substitution element as shown in Fig. 3 by the $Mg_{0.5}Ti_{0.5}Ni$ compound (capacity retention of 70% after 15 cycles). However, it has a cost on the maximal capacity of the electrode, which is 312 mAh g^{-1} for $Mg_{0.5}Ti_{0.5}Ni$ compared to 415 mAh g^{-1} for $Mg_{0.9}Ti_{0.1}Ni$ material.

Our work on quaternary Mg–Ni–Ti–Al materials has shown that it is possible to improve the electrode cycle life without significantly decreasing the Mg content of the alloy. Indeed, as seen in Fig. 3, the degradation rate of the quaternary $Mg_{0.9}Ti_{0.1}NiAl_{0.05}$ upon cycling is significantly lower than measured with the ternary $Mg_{0.9}Al_{0.1}Ni$ and $Mg_{0.9}Ti_{0.1}Ni$ alloys despite the same Mg stoichiometry. This confirms the existence of a synergistic effect between Ti and Al for improving the cycle life of the MgNi-based electrode. Note that, through the evaluation of various Mg–Ni–Ti–Al materials (not shown), the Ti/Al atomic ratio must be higher than 1 for observing such a synergistic effect. We have recently shown that this cooperative effect between Ti and Al on the electrode cycle life has two origins [46]: (i) an improvement of the alloy corrosion resistance due to the formation of a more efficient $Al_2O_3 + TiO_2$ protective layer than either TiO_2 or Al_2O_3 alone for limiting $Mg(OH)_2$ formation, and (ii) an increase in its resistance to pulverization upon hydrogen charging due to an improvement of its mechanical properties (lower hardness).

3.6. Influence of the charge input

The influence of the charge input value on the capacity decay of the quaternary $Mg_{0.9}Ti_{0.1}NiAl_{0.05}$ electrode was studied by varying the charge input value from 200 to 300 mAh g^{-1} (Fig. 4). For all the charge input values, the initial discharge capacity is higher than the charge input. This additional discharge capacity is assumed to be related to the irreversible anodic formation of oxides/hydroxides (e.g. $Mg(OH)_2$, TiO_2, Al_2O_3) during the first discharge procedure. From the second cycle, no capacity decay is observed if the charge input is equal to or lower than 260 mAh g^{-1}. For a charge input of 280 mAh g^{-1}, slow capacity degradation is observed from the 5th cycle while at 300 mAh g^{-1}, the capacity decay appears immediately. Actually, for higher charge inputs than 260 mAh g^{-1}, it is assumed that extended particle pulverization occurs, which breaks the passive surface layer formed during the first charge/discharge cycle. This creates unprotected fresh surfaces and consequently, leads to the electrode capacity degradation. This demonstrates that the calendar corrosion is not the main electrode degradation process and thus, the key issue to obtain stable Mg-based electrodes is to limit their pulverization upon cycling.

On the basis of the charge input threshold ($C_{threshold}$) of 260 mAh g^{-1} and assuming that the charge Faradaic efficiency is 100%, the maximum hydrogen content absorbed by the $Mg_{0.9}Ti_{0.1}NiAl_{0.05}$ particles before their pulverization corresponds to an atomic hydrogen-to-metal ratio (H/M) of 0.41. For MgNi and $Mg_{0.9}Ti_{0.1}Ni$ materials, the maximum H/M value before degradation is lower (i.e. 0.34 and 0.38, respectively) [46]. This confirms the better pulverization resistance of the quaternary $Mg_{0.9}Ti_{0.1}NiAl_{0.05}$ compared to MgNi and $Mg_{0.9}Ti_{0.1}Ni$. Note that these H/M values are much higher than the maximal H/M value in the α-phase, which is typically lower than 0.1. This might reflect a gradual volume expansion upon

Table 2
Electrode performance of $Mg_{0.9}Ti_{0.1}NiAl_{0.05}$ with respect to the particle size

Particle size (μm)	C_1 (mAh g^{-1})	C_{15}/C_1 (%)	$C_{threshold}$ (mAh g^{-1})	$C_{threshold}/C_1$ (%)
<20	304	31	140	46
20–75	403	53	240	60
75–106	416	66	280	67
106–150	420	72	280	67
>150	449	72	300	67
As-milled	404	67	260	64

hydrogen absorption of our MgNi-based materials due to their amorphous structure in contrast to crystalline alloys such as $LaNi_5$-based compounds characterized by an abrupt α-to-β lattice expansion [47].

3.7. Powder sieving

The influence of the particle size on the cycling performance of $Mg_{0.9}Ti_{0.1}NiAl_{0.05}$ is presented in Table 2. For this study, the as-milled powder was sieved in five fractions: <20, 20–75, 75–106, 106–150 and >150 μm. The mass yield of these particle size fractions was 23, 39, 10, 8 and 20%, respectively.

It appears that the initial discharge capacity is higher as the particle size increases. It may reflect the decrease of the electrode oxidation due to a lower surface area in contact with the electrolyte as the particle size increases. Then, because the electrode with the larger particles has a larger fraction of un-oxidized (i.e. active) material, it is not surprising that it displays a larger initial discharge capacity. The electrode cycle life is also improved by increasing the particle size. Indeed, the capacity retention after 15 cycles (C_{15}/C_1) is 72% for >150 μm particles compared to 31% for <20 μm particles. This confirms that the electrode oxidation is accelerated with decreasing the particle size. It is in accordance with our recent study of the influence of particle size on the MgNi electrode performance [48]. Moreover, the charge input threshold inducing capacity degradation ($C_{threshold}$) increases as the particle size increases. This may result from an increase of the proportion of active material as indicated previously. However, the $C_{threshold}$ to C_1 ratio increases from 46% for <20 μm particles to 67% for >75 μm particles. These values can be considered, in a first approximation, as the maximum states of charge that the electrodes can support without continuous powder pulverization during cycling. The fact that this value increases with the particle size seems to indicate that the electrode resistance to pulverization increases as the particle size increases. A possible explanation is that the volume change induced by hydrogen charging/discharging is easier to relax with the large particles due to their larger proportion of void compared to the small particles presenting a more compact morphology [48].

3.8. Optimized electrode

Finally, we have developed an optimized Mg-based electrode made of amorphous $Mg_{0.9}Ti_{0.1}NiAl_{0.05}$ alloy with particles larger than 150 μm. For a charge input limited at 300 mAh g^{-1}, this optimized electrode displays a capacity decay rate as low as that observed with a commercial $LaNi_5$-type material ($MmNi_{3.6}Co_{0.8}Al_{0.35}Mn_{0.25}$) tested under the same conditions. Indeed, as shown in Fig. 5, the two electrodes exhibit a similar capacity decay rate of ca. 0.2% per cycle from the second cycle. Moreover, the $Mg_{0.9}Ti_{0.1}NiAl_{0.05}$ electrode maintains a discharge capacity ~5–10% higher than that of the commercial $LaNi_5$-based material. In addition, the $Mg_{0.9}Ti_{0.1}NiAl_{0.05}$ electrode is cheaper in terms of material cost than the $LaNi_5$-based compounds because of the absence of expensive elements such as Co. However, the industrial cost of the ball milling and powder sieving procedures has to be evaluated for confirming the economic advantage of this Mg-based material compared to the commercial $LaNi_5$-based materials.

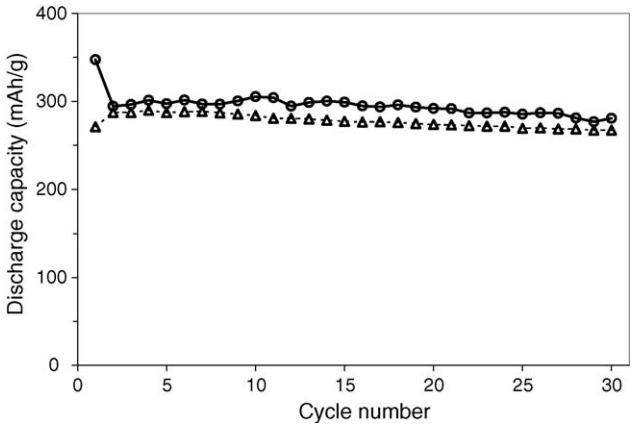

Fig. 5. Cycling discharges capacities of $Mg_{0.9}NiTi_{0.1}Al_{0.05}$ electrode with particles larger than 150 μm (◯) and $LaNi_5$-based material (Δ). Charge input = 300 mAh g^{-1}.

Note that the previous cycle life tests were performed using an open half-cell which is very different from a commercial Ni-MH battery. In a real Ni-MH battery, the MH electrode capacity is higher than the nickel hydroxide electrode capacity and thus, the depth of charge of the MH electrode would be limited in order to prevent its pulverization as done previously. Moreover, the high compression used in real battery may further reduce the electrode pulverization. On the other hand, oxygen produced at the positive electrode during overcharge reacts on the surface of the MH. This oxygen-recombination process accentuates MH surface oxidation and thus, it may affect significantly the MH cyclability.

In addition, the high-rate dischargeability of the Mg-based alloys is presently too low. For instance, the high-rate dischargeability denoted as the ratio of the maximal discharge capacity measured at a current density of 200 mA g^{-1} to the maximal discharge capacity measured at 20 mA g^{-1} (C^{200}/C^{20}) is 58% for $Mg_{0.9}Ti_{0.1}NiAl_{0.05}$ compared to 75% for commercial $LaNi_5$-based alloy tested under the same conditions. This limits their use for high power applications (e.g. hybrid electric vehicles). This is assumed to be essentially related to the high stability of the Mg-based hydride phase, which is characterized by a hydrogen plateau pressure around 10^{-4} MPa at room temperature [49,50] compared to 10^{-1} MPa for AB_5-type materials [47].

These concerns have to be solved for potential use of Mg-based alloys in real applications.

Acknowledgements

This work has been financially supported by the National Sciences and Engineering Research Council (NSERC) of Canada and the "Fond de Recherche sur la Nature et les Technologies" of Quebec.

References

[1] S. Ruggeri, C. Lenain, L. Roué, H. Alamdari, G. Liang, J. Huot, R. Schulz, Mater. Sci. Forum 11 (2001) 63.
[2] W. Liu, Y. Lei, D. Sun, J. Wu, Q. Wang, J. Power Sources 58 (1996) 243.
[3] N.H. Goo, J.H. Woo, K.S. Lee, J. Alloys Compd. 288 (1999) 286.
[4] T. Abe, T. Tachikawa, Y. Hatano, K. Watanabe, J. Alloys Compd. 330–332 (2002) 792.
[5] S. Ruggeri, L. Roué, J. Huot, R. Schulz, L. Aymard, J.M. Tarascon, J. Power Sources 112 (2002) 547.
[6] S. Ruggeri, L. Roué, J. Power Sources 117 (2003) 260.
[7] S.C. Han, P.S. Lee, J.Y. Lee, A. Zuttel, L. Schlapbach, J. Alloys Compd. 306 (2000) 219.
[8] G.L. Song, A. Atrens, Adv. Eng. Mater. 1 (1999) 11.
[9] J.E. Gray, B. Luan, J. Alloys Compd. 336 (2002) 88.
[10] A.U. Simaranov, S.L. Marshakov, Y.N. Mikhailovskii, Protect. Met. 28 (1992) 576.
[11] ASM Handbook: Corrosion, vol. 13, ASM International, 1987, pp. 740–754.
[12] A. Kolics, A.S. Besing, A. Wieckowski, J. Electrochem. Soc. 148 (2001) B322.
[13] C.Y. Wang, P. Yao, D.H. Bradhurst, H.K. Liu, S.X. Dou, J. Alloys Compd. 285 (1999) 267.
[14] J. Chen, D.H. Bradhurst, S.X. Dou, H.K. Liu, J. Alloys Compd. 280 (1998) 290.
[15] J.L. Luo, N. Cui, J. Alloys Compd. 264 (1998) 299.
[16] T. Sakai, H. Ishikawa, K. Oguro, C. Iwakura, H. Yoneyama, J. Electrochem. Soc. 134 (1987) 558.
[17] B.S. Haran, B.N. Popov, R.E. White, J. Electrochem. Soc. 145 (1998) 3000.
[18] R.C. Ambrosio, E.A. Ticianelli, J. Electrochem. Soc. 150 (2003) E438.
[19] M.S. Wu, H.R. Wu, Y.Y. Wang, C.C. Wan, J. Alloys Compd. 302 (2000) 248.
[20] H.J. Park, N.H. Goo, K.S. Lee, J. Electrochem. Soc. 150 (2003) A1328.
[21] J.S. Kim, C.R. Lee, J.W. Choi, S.G. Kang, J. Power Sources 104 (2002) 201.
[22] J.J. Jiang, M. Gasik, J. Power Sources 89 (2000) 117.
[23] C. Iwakura, H. Inoue, S. Nohara, R. Shin-ya, S. Kurosaka, K. Miyanora, J. Alloys Compd. 330–332 (2002) 636.
[24] Q.M. Yang, M. Ciureanu, D.H. Ryan, J.O. Ström-Olsen, J. Alloys Compd. 274 (1998) 266.
[25] W.K. Choi, T. Tanaka, R. Miyauchi, T. Morikawa, H. Inoue, C. Iwakura, J. Alloys Compd. 299 (2000) 141.
[26] H.K. Liu, N. Cui, B. Luan, J. Chen, S.X. Dou, D.H. Brahurst, J. N. Mater. Electrochem. Syst. 1 (1998) 77.
[27] M. Zhu, Z.M. Wang, C.H. Peng, M.Q. Zeng, Y. Gao, J. Alloys Compd. 349 (2003) 284.
[28] S.S. Han, N.H. Goo, W.T. Jeong, K.S. Lee, J. Power Sources 92 (2001) 157.
[29] S.S. Han, N.H. Goo, K.S. Lee, J. Alloys Compd. 360 (2003) 243.
[30] X.B. Yu, Z. Wu, B.J. Xia, N.X. Xu, J. Electrochem. Soc. 151 (2004) A1468.
[31] T. Kohno, M. Kanda, J. Electrochem. Soc. 144 (1997) 2384.
[32] X. Jianshe, L. Guoxun, H. Yaoqin, D. Jun, W. Chaoqun, H. Guangyong, J. Alloys Compd. 307 (2000) 240.
[33] S. Nohara, K. Hamasaki, S.G. Zhang, H. Inoue, C. Iwakura, J. Alloys Compd. 280 (1998) 104.
[34] C. Iwakura, R. Shin-ya, K. Miyanohara, S. Nohara, H. Inoue, Electrochim. Acta 46 (2001) 2781.
[35] C. Lenain, L. Aymard, L. Dupont, J.M. Tarascon, J. Alloys Compd. 292 (1999) 84.
[36] J. Chen, P. Yao, D.H. Bradhurst, S.X. Dou, H.K. Liu, J. Alloys Compd. 293–295 (1999) 675.
[37] H.T. Yuan, E.D. Yang, H.B. Yang, B. Liu, L.B. Wang, R. Cao, Y.S. Zhang, J. Alloys Compd. 291 (1999) 244.
[38] H. Ye, Y.Q. Lei, L.S. Chen, H. Zhang, J. Alloys Compd. 311 (2000) 194.
[39] Y. Zhang, B. Liao, L.X. Chen, Y.Q. Lei, Q.D. Wang, J. Alloys Compd. 327 (2001) 195.
[40] Y. Zhang, S.K. Zhang, L.X. Chen, Y.Q. Lei, Q.D. Wang, Int. J. Hydrogen Energy 26 (2001) 801.
[41] Y. Zhang, L.X. Chen, Y.Q. Lei, Q.D. Wang, Electrochim. Acta 47 (2002) 1739.
[42] S.C. Han, J.J. Jiang, J.G. Park, K.J. Jang, E.Y. Chin, J.Y. Lee, J. Alloys Compd. 285 (1999) L8.
[43] Y. Zhang, Y.Q. Lei, L.X. Chen, J. Yuan, Z.H. Zhang, Q.D. Wang, J. Alloys Compd. 337 (2002) 296.
[44] Q.D. Wang, Y. Zhang, Y.Q. Lei, J. Alloys Compd. 356–357 (2003) 784.
[45] J.W. Liu, H.T. Yan, J.S. Cao, Y.J. Wang, J. Alloys Compd. 392 (2005) 300.
[46] C. Rongeat, L. Roué, J. Electrochem. Soc. 152 (2005) A1354.
[47] P.H.L. Notten, J.L.C. Daams, R.E.F. Einerhand, J. Alloys Compd. 210 (1994) 233.
[48] C. Rongeat, L. Roué, J. Power Sources 132 (2004) 302.
[49] S. Ruggeri, L. Roué, G. Liang, J. Huot, R. Schulz, J. Alloys Compd. 343 (2002) 170.
[50] S. Orimo, H. Fujii, Appl. Phys. A 72 (2001) 167.